ELSEVIER

Journal of Materials Processing Technology 100 (2000) 179–187

Journal of Materials Processing Technology

www.elsevier.com/locate/jmatprotec

The influence of parameter settings on cathodic self-etching during aluminum welding

Ph.D. Américo Scotti*, Ph.D. Jair Carlos Dutra, Ph.D. Valtair Antonio Ferraresi

Laboratório para o Desenvolvimento de Processos de Soldagem, Departamento de Engenharia Mecânica, Universidade Federal de Uberlândia, 38400-902 Uberlândia, MG, Brazil

Received 22 September 1998

Abstract

Cathodic self-etching is a mechanism that has been used for a long time to make feasible the GTA welding of aluminum, by cleaning the metal surface in real time. The use of power supplies with rectangular wave AC output has extended the efficiency of the phenomenon. The objective of this work is to gain further insight into this matter. A study of the influence of the power source output parameters and travel speed on cathodic etching and, consequently, on welding geometry and arc stability is presented. An experimental design based in the robust design technique was applied to make the number of experiments affordable. The obtained tendencies were confirmed by validation experiments and comparison with the results of other authors: The results suggest the beneficial effect of a short electrode positive duration and increasing travel speed on oxide cleaning. Too effective cathodic etching leads to arc instability during polarity reversal. The negative electrode amplitude and duration does not govern this aspect, yet they govern the bead geometry. Finally, a theoretical explanation of the phenomena is proposed.

Keywords: Aluminum; Welding; Cathodic etching; Experimental design

1. Introduction

It is well known that the efficient thermionic emission[1] practiced by the gas tungsten arc welding process (GTAW) with direct current-electrode negative (DCEN) does not work so easily for aluminum welding. Aluminum alloys form a refractory surface oxide, which is responsible for the high oxidation resistance of these alloys. This surface oxide layer, the fusion temperature of which is much higher than that of the metal, prevents the heat to flow to the underlying metal and makes joining more difficult [3]. Aluminum alloy GTAW with DCEN is not possible unless the oxides are previously removed and/or a more thermally efficient shielding gas is used, such as helium or a helium–argon mixture with at least 65% [4].

On the other hand, when this type of material is welded under electrode positive (DCEP) conditions where the aluminum plate becomes the electron emitter, a workpiece oxide self-cleaning phenomenon is assumed to take place. The phenomenon of oxide self-cleaning, based on cathodic etching, is explained on the basis of the electron emission, as follows:

Electron emission from non-thermionic workpiece materials (such as aluminum) is only possible by a phenomenon called "field emission" or "non-thermionic cathode". There are at least three types of non-thermionic cathodes [2]: the vapor type, which forms on unfilmed metal, the tunneling type, which forms on thin (<10 nm) oxide films, and the switching type, which forms on thicker oxide films. Concentrating on the case of aluminum GTAW with the plate as cathode, it is suggested that positive ions condense on the oxide surface and set-up a high electrical field. In the case of thin films, if the field is higher than about 10^9 V/m, electrons may tunnel through the film and generate an emitting site. For thick films a phenomenon known as switching makes the film locally conducting [2].

Thus, field emission in aluminum alloys is the result of a very high voltage gradient between the metal cathode and a

* Corresponding author. Tel.: +55-34-239-4192; fax: +55-34-239-4206.
E-mail address: ascotti@ufu.br (A. Scotti).

[1] Thermionic emission occurs when a refractory cathode is heated to a sufficiently high temperature to emit electrons. Only materials with boiling points of at least 4000 K, such as tungsten (the boiling point of iron is 3343 K), can work as thermionic cathode [1]. The addition of some oxides, such as of thorium, zirconium, and lanthanum, allows tungsten electrodes to operate below its melting point, due to their lower work function [2].

0924-0136/00/$ – see front matter
PII: S0924-0136(00)00436-2

positively charged oxide layer. The existence of this positively charged oxide layer is due to incident positive ions onto the surface oxides, which are formed by reaction between oxygen and the workpiece elements; the oxides are believed to act as a source of electrons because they usually have a lower work function than the correspondent metals [1]. It appears that this mentioned high voltage gradient happens because the electrons concentrate in some sites (spots). These individual emitting sites are of approximately 1 nm in diameter and move about on the cathode surface [2].

This locally generated temperature is sufficient for melting or evaporating the oxides, which, by surface tension or vaporization, are removed from the weld pool surface, causing the oxide self-cleaning. There are other theories by means of which this cathodic etching effect can be explained [4]. In one theory, the electrons striking the workpiece at high velocity tear off the oxide skin and break it down into very small particles, whilst in another theory, the ions striking the workpiece have sufficient energy to shatter the oxide skin. Evidence for this theory would be that the cleaning effect with an inert gas of high relative atomic mass (argon) is more pronounced than with a lighter gas (helium).

As seen, aluminum and its alloys can be defined as non-thermionic cathodes characterized by a mobile cathode spot [5]. In Jönsson et al.'s review paper [1], this mobility arises from a continuous formation and decay of several small electron-emitting sites (cathode spots). The site lifetime for thick oxide films on mild steel is reported as being as low as 1 ns. The emitting sites are also said to move outwards toward fresh oxide and to consume it at a certain rate. The area over which the oxide is removed increases with an increase in the cathode voltage drop. The mobile cathode spot often leaves visible traces on the metal surface where oxide or metal has been removed [2]. Modenesi and Nixon [6] state in their review that the arc would consume a 0.2–0.5 μm thick oxide layer at a rate of 0.6 mm^2/s. For the case of an aluminum workpiece material, it has been shown [1] that the presence of a relatively thick oxide layer tends to restrict the mobility of the cathode spot. It can be assumed that the wider the visible traces on the metal surface, the more efficient the oxide self-cleaning action by the DCEP condition.

From the details mentioned above it can be inferred that arc stability in aluminum GTAW DCEP is related to electron emission facility by the cathode. If there is little oxide on the aluminum surface, there will be no electron emission if cathode is the plate. The arc will be wandering on the plate surface looking for oxides (this is characterized by an arc trace or sputter marks on the metal surface). This mobility of non-thermoionic cathode spots might cause arc instability.

Lancaster [2] cites that, for direct movement, the trace width is approximately proportional to the current and inversely proportional to the velocity, provided that the cathode oxide is thicker than about 25 nm. This is not true for a well-polished cathode. Norrish and Ooi [7] found in their experiments that both the weld bead width and the sputtered zone width (the electronically cleaned area) increase with current, although at lower currents the sputtered zone width is greater for increasing electrode positive duration. Barhorst's results [8] show that the primary variable for determining the cleaning action width is the DCEP polarity current. The DCEP time duration has considerably less influence on the cleaning action. Rehfeldt et al. [9] consider that both the sputtered zone width and the changing appearance of the surface of the zone are an expression of the motion of the arc attachment point. They detected that the polarity reversing frequency affects these two criteria; whereas with low frequencies, up to 100 Hz, a uniformly diffuse surface appearance is present, with the frequency increased to 200 Hz, a differently structured, narrow core, region is formed. Above 2 kHz, a decrease in the uniformity of the zone begins.

Regarding bead geometry, Reis [10] showed in former work that current levels for both polarities are more significant than the respective duration times on bead geometry formation. It was also shown that a better arc stability is achieved if the $t+$ is very short and if the $t-$ assumes a longer value, i.e., stability is not satisfactory for a utterly cathodic cleaning. It was observed that the $t-$ effect on geometry appeared only for $t-$ longer than 6 ms. There is a straight relationship between welding speed (TS) and feeding speed (WFS) and this relationship must be followed for obtaining sound beads inside a groove. Higher TS also seemed to lead to a more stable arc.

However, despite all knowledge found in the current literature, there is very little data concerning the optimum practical parameter setting. Considering that oxide surface cleaning is an essential condition for aluminum alloy GTAW, it is not yet totally understood if the mobility of the non-thermionic cathode spots, because of the DCEP oxide self-cleaning action, can lead to an arc instability. It is not clear either what the influence of the sputter mark on welding geometry is. Therefore, the purpose of this work is to study the influence of some variables of rectangular-wave AC GTAW on the performance of the process during aluminum welding, focusing on aluminum surface cleaning by cathodic self-etching phenomena. Instead of studying the phenomenon itself, for which sophisticated techniques are demanded, the approach proposed is an indirect study through its consequence on weld arc stability and bead formation.

2. Experimental procedure

Some experimental procedures were proposed to investigate the influence of the negative polarity duration ($t-$), current amplitude ($I+$ and $I-$) and travel speed (TS) on the arc stability and parent metal fusion behavior. The welds were carried out as bead-on-plate and no wire feeding was used. This approach had the purpose of isolating the influ-

ence of joint preparation and the wire composition upon the overall arc performance.

2.1. Welding conditions and assessment means

Some welding conditions were maintained as constants along all tests as follows.

Bead-on-plate welds were deposited longitudinally on aluminum plates (Al 1060) of approximate dimensions 150 mm×70 mm×6 mm. Two stringer beads were deposited on each plate, the centerlines of which were situated 10 mm away from the plate centerline. The plates were precleaned with acetone. No other mechanical or chemical cleaning was employed.

The beads were carried out under mechanized conditions (an electronically controlled linear carriage). A water-cooled torch was positioned normal to the test plate surface, with a 3.25 mm diameter electrode (AWS WTh 2%), with 30 mm extension (stick-out) and 60° tapered end. A 2 mm long arc length was employed in all tests. The electrode was ground in a W tapering machine before each test (run). Commercially pure argon was used as the shielding gas at the rate of 18 l/min.

For these tests an electronically controlled (secondary chopped) multiple-process welding power source was used. One special characteristic of this power source, concerning this work, is the capability of individual digital setting for the AC wave form parameters, i.e., $I+$, $I-$, $t+$ and $t-$. Up and down slope, shielding gas pre-purge and post-purge, are other machine capabilities. This power source provides also a very short 600 V capacitor discharge every time the current goes from the negative period to the positive period.

The arc voltage and current signals were recorded directly into a microcomputer data acquisition board. The signal acquisition was made at a rate of 12 kHz at each channel, at 8 bit, for 9.4 s (resolutions of 0.22 A for current and of 0.02 V for arc voltage). Arc voltages were measured between the workpiece and the contact-tip of the torch. A "Hall effect" probe in series with the arc enabled accurate monitoring of the current waveform. A visualization software permitted the analysis of the signals (V vs. t and I vs. t) after welding (including zoom capability), with a time resolution of approximately 21 ms (inverse of the acquisition frequency plus the screen resolution, which in turn is the total acquisition time divided by 600 pixels). The mean values of the amplitude and periods of current and voltage were obtained by direct measurement of the signal traces (from three sampling cycles, at approximately 1000, 4000 and 7000 ms). The results are presented as the average value of the three samples. More details of the experimental set-up can be found elsewhere [11].

To evaluate the effect of the variables on the process performance, two classes of parameters were chosen. The first class is related to geometric aspects of the beads, i.e., width (W), penetration (P) and fusion area (FA). This first aspect was quantified by a direct measurement (vernier caliper) on the bead (the mean of at least 10 measurements). For the two other aspects, two transverse sections of each test plate were randomly cut (50 mm away from each other) and prepared for metallography. After etching (Turcker's reagent), the geometric parameters were measured using a digital image analyzer.

The second class concerns stability aspects. As arc stability is not an easily quantified property, two criteria were proposed. The first one was the sputtering zone width (SZW); the wider the zone, the more mobile the cathodic spots (less stability). As the sputtering zone width can be influenced by the weld pool width, the parameter used to quantify this criterion cleared this effect by diminishing the bead width from the sputtering zone width. Better stability would be related to a lower net sputtering zone width (SZWnet). A second attempt, an even more subjective criterion, was to give a grade to each weld based on the operators feelings and visual observations. A GRADE 2 is due to an arc with no extinguishing and/or no wandering. A GRADE 0 is given for an arc with significant observations of arc wandering and extinguishing, whereas for an intermediate behavior for GRADE 1 is reserved.

2.2. Experimental design

Beforehand, three welding variables (factors) were chosen for this study, i.e., current amplitudes ($I+=I-$), travel speed (TS) and negative polarity duration ($t-$). These variables were found to be the most significant ones in previous work [10]. The initial experimental planning was made for three levels of I, three levels of TS and four levels of $t-$. Taking into account the number of factors and levels (degrees of freedom equal to 8), the experimental design was based on the robust design technique [12]. An L'16 orthogonal array was selected.

In this matrix experiment, the columns of the array are mutually orthogonal. Here orthogonality is interpreted in the combinatory sense, i.e., for any pair of columns, all combinations of factor levels occur and they occur an equal number of times. This is called balancing property [12]. The L'16 orthogonal array is a standard array of Taguchi and Wu planned for five 4-level factors. To adequate the desired number of factors and level to this matrix, three changes were implemented subjectively.

1. The number of variables was increased (I was split into $I+$ and $I-$). This approach was implemented instead of using an empty column to improve the experimental efficiency (a gain of information about an additional factor without spending any more resources).
2. The number of levels of TS was increased to 4.
3. The dummy level technique [12] was applied to the $I+$ and $I-$ variables, so that the number of their levels could be kept as 3 (a greater number of levels could make the values statistically confounding, since the range of current for a given electrode diameter is limited).

Table 1
Modified L'16 orthogonal array experimental design

Run	Factors			
	A	B	C	D
1	A_1	B_1	C_1	D_1
2	A_1	B_2	C_2	D_2
3	A_1	B_3	C_3	D_3
4	A_1	B'_2	C_4	D_4
5	A_2	B_1	C_2	D_4
6	A_2	B_2	C_1	D_3
7	A_2	B_3	C_4	D_2
8	A_2	B'_2	C_3	D_1
9	A_3	B_1	C_3	D_2
10	A_3	B_2	C_4	D_1
11	A_3	B_3	C_1	D_4
12	A_3	B'_2	C_2	D_3
13	A'_2	B_1	C_4	D_3
14	A'_2	B_2	C_3	D_4
15	A'_2	B_3	C_2	D_1
16	A'_2	B'_2	C_1	D_2

Table 1 presents the resulting experimental design, where the capital letters from A to D are the factors $I-$, $I+$, TS and $t-$, respectively, and the numerals from 1 to 4 are the levels. $A_4=A_2$ (A'_2) and $B_4=B_2$ (B'_2) were taken as the dummy levels. The following levels were chosen as nominal values (values to be adjusted in the power source) for the factors:

- $A=I-$ (current value during negative period)

  $A_1=150$ A; $A_2=180$ A; $A_3=210$ A

- $B=I+$ (current value during positive period)

  $B_1=150$ A; $B_2=180$ A; $B_3=210$ A

- C=TS (travel speed)

  $C_1=10$ cm/min; $C_2=18$ cm/min; $C_3=26$ cm/min; $C_4=34$ cm/min

- $D=t-$ (duration of negative period)

  $D_1=5$ ms; $D_2=10$ ms; $D_3=15$ ms; $D_4=20$ ms

Following the experimental design from Table 1 and keeping the nominal $t+=2$ ms and arc length=2 mm, the welds were carried out in a random order. Table 2 shows the actual parameters used (the averaged value from the monitoring system) in each run, excepting for TS, which is the adjusted value (nominal).

It can be seen in Table 2 that for a given condition, the standard deviations of the monitored parameters were low, showing how good was the power supply output. However, one can also see a big difference between the set values and the actual values. As the errors were systematic, the cause was attributed to a lack of calibration of the power supply. It is important to remember that, due to the random order, each run had the set adjusted again, i.e., the setting knobs of the power supply were always altered for each new run.

It is worth mentioning that the runs 1, 10, 11, 15 and 16 were troublesome in striking and maintaining the arc at the beginning of the weld. After plate heat stabilization, the arcs ran more steadily. One can notice that these runs are characterized by a low $t-$ and/or low TS.

In order to validate the outcome analysis from the above experimental design, other experiments were planned and carried out. The first two were replications of run 6 (run 6B) and run 12 (run 12B). The other was a modification of run 10, where the $I+$ and $I-$ sets were inverted (run 20). As run

Table 2
Actual welding parameters[a] used in the experimental design

Run	$I-$ (A)	$I+$ (A)	$t-$ (ms)	$t+$ (ms)	TS (cm/min)	$V-$ (V)	$V+$ (V)
1	153±3	158±0	4.90±0.02	1.82±0.11	10	7.3	21.8
2	181±1	158±0	9.80±0.05	1.79±0.05	18	8.2	19.8
3	213±0	158±0	15.37±0.77	1.64±0.14	26	8.8	19.8
4	183±0	158±0	19.91±0.02	1.71±0.10	34	9.3	18.0
5	150±0	189±0	19.90±0.02	1.68±0.11	18	9.6	17.1
6	182±0	188±0	14.87±0.04	1.76±0.03	10	9.5	19.5
7	212±2	189±0	9.78±0.04	1.64±0.16	34	8.5	19.2
8	185±1	188±0	4.83±0.01	1.70±0.08	26	7.8	19.2
9	152±0	219±0	9.78±0.04	1.73±0.08	26	10.6	17.8
10	183±5	219±0	4.78±0.04	1.81±0.08	34	7.7	20.6
11	215±5	219±0	20.01±0.00	1.67±0.02	10	9.8	19.6
12	182±0	219±0	14.76±0.00	1.79±0.04	18	10.8	18.4
13	152±0	188±0	14.95±0.04	1.83±0.00	34	9.9	18.4
14	181±1	188±0	19.79±0.06	1.77±0.09	26	9.5	17.8
15	212±2	188±0	4.67±0.01	1.69±0.07	18	7.4	22.4
16[b]	182±1	188±0	9.79±0.01	1.74±0.06	10		

[a] The average of $I+$, $I-$, $t+$, $t-$, $V-$, and $V+$ represents the mean and standard deviation of three values (cycles). These values themselves were taken as the mean of several samples (minimum 15) within each cycle. The maximum dispersion within one cycle reached ±2 A for $I-$ and 8 A for $I+$. The TS values are the setting value (no monitoring).

[b] The data acquisition was missed. The values refer to the average value of the other runs with the same settings. Considering the very low standard deviation, it can be assumed that the values are representative.

Table 3
Actual welding parameters used in the experimental design for validation

Run	$I-$ (A)	$I+$ (A)	$t-$ (ms)	$t+$ (ms)	TS (cm/min)	$V-$ (V)	$V+$ (V)
6B[a]	182±1	188±0	15.00±0.20	1.74±0.06	10		
12B	188±0	211±7	14.79±0.06	1.49±0.07	18	9.2	18.6
20	219±0	181±0	4.86±0.04	1.78±0.04	34	7.6	19.8
20B	158±0	182±1	4.70±0.07	1.69±0.15	34	7.4	20.6
20C	158±0	182±1	8.70±0.04	1.70±0.11	34	8.7	19.0
14B	190±0	183±0	24.59±0.00	1.82±0.11	26	10.0	17.1
14C	188±0	181±0	29.70±0.00	1.85±0.01	26	9.8	17.0
14D	189±0	181±2	39.28±0.06	1.83±0.00	26	10.8	17.6
16B[a]	182±1	188±0	9.79±0.01	1.74±0.06	20		
16C	190±0	182±1	9.66±0.00	3.64±0.04	10	7.8	22.4

[a] The data acquisition was missed. The values refer to the average value of the other runs with the same settings. Considering the very low standard deviation, it can be assumed that the values are representative.

10 had shown arc-strike problems, run 20 was started on a heated aluminum tab placed face-to-face to the test-plate. This approach provided a better arc maintenance when the arc went through the test-plate (a further run without the hot tab brought the arc-striking problem back). Table 3 presents the input and output parameters of these experiments, together with those of other supplementary experiments, the objectives of which are explained below.

In order to isolate the effect of the current values, run 20 was replicated, by setting $I-$ to a lower value, and named run 20B. Run 3 was also replicated, but after 1/3 of the weld length had been carried out, the $I+$ was decreased to 150 A. After 2/3 of the total length, the $I+$ was further reduced to 120 A (set values).

For checking the isolated effect of the $t-$, run 20B was replicated (run 20C) using a longer $t-$. A series of runs with longer $t-$ (run 14B, 14C and 14D) was also produced taking run 14 as a base (40 ms was the power source limit). It was noted that a black line appeared on the bead centerline of run 14C ($t-$ equals 30 ms), resembling oxides. At longer $t-$ (run 14D), this line became more pronounced.

The effect of the TS and the duration of $t+$ were verified by taking run 16 and either increasing the TS (run 16B) or increasing $t+$ to 4 ms (run 16C).

3. Results and analyses

Table 4 presents the responses from the experimental procedure and supplementary runs.

The significance of each factor to the responses was found using Taguchi's approach for standard orthogonal arrays [12]. A summary of the analysis of variance (ANOVA) for runs 1–16 is shown in Table 5, in which the factors with a high F-number and F significance of at least 5% are considered to control the responses. To see how each factor influences the responses (directly or inversely proportional), a plot of means technique was employed.

Two criteria were proposed to analyze the stability aspects (SZWnet and GRADE). Table 5 shows that the SZWnet and GRADE seem to be affected by the factors in the same way, which means that they are correlated with each other and that either of them can be used as a stability criterion. Considering that the GRADE criterion is very subjective, SZWnet was chosen as the main stability criterion for further analysis. Then, the arc stability seems to be highly influenced by $t-$ and TS, and the $I+$ and $I-$ values play an insignificant role.

Concerning the geometric aspects of the beads, one can see that the W increases as TS decreases and $I-$ and $t-$ increase. P is not significantly influenced by TS, but it is also governed by $I-$ and $t-$ in a straight relationship. The effect of $t-$ is reduced in the formation of the FA. $I+$ seems not to play any role in the welding geometry for the given duration.

Despite not being in the scope of this work, the $V+$ and $V-$ values were also verified. As seen in Table 5, $t-$ is the most significant factor for both (longer $t-$ demands higher $V-$ and lower $V+$). The $I+$ and $I-$ values secondarily affect $V+$ and $V-$, respectively.The approach for the experimental design and analysis applied in this work assumes that all of the main factors are independent and that there is no significant interaction amongst them. To verify this assumption, plots of the interactions between each pair of factors were traced, as illustrated in Fig. 1, where an interaction of the antisynergistic type is the one that usually breakdown the principle of additivity of the main factors [12]. Most inter-

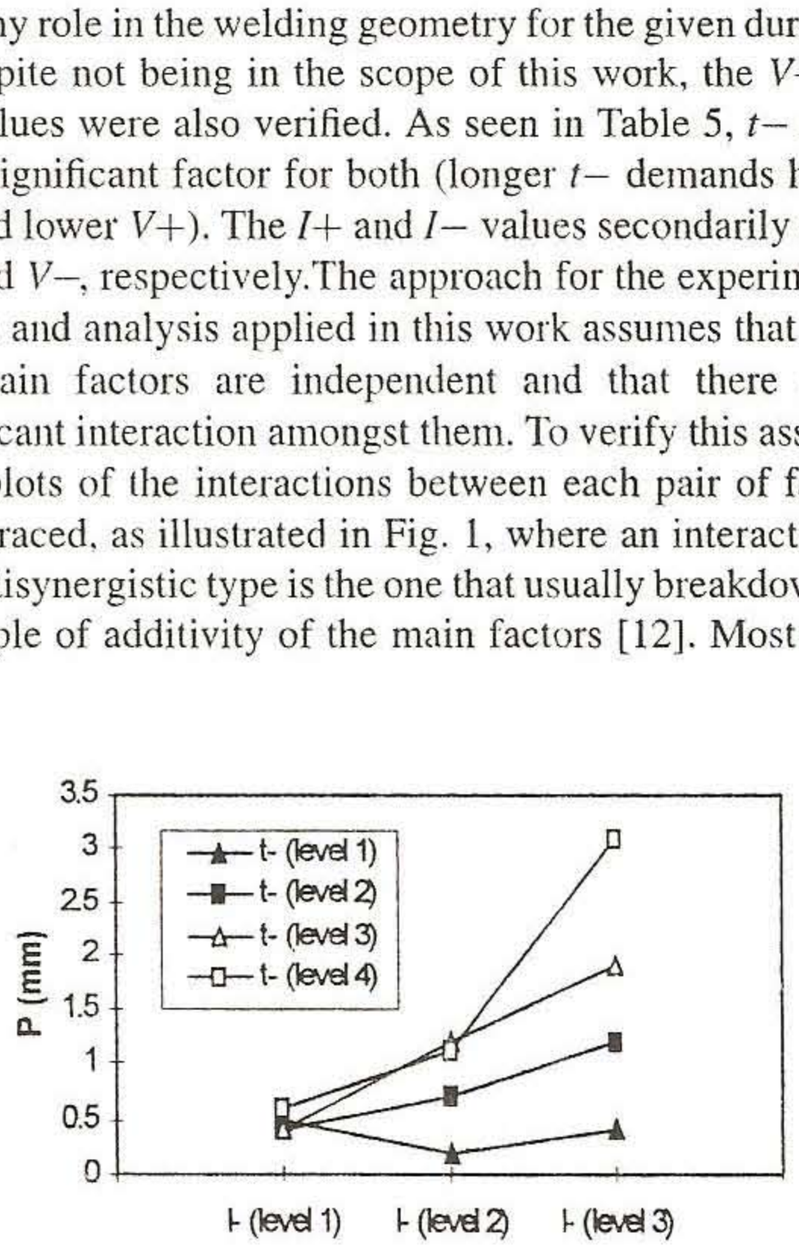

Fig. 1. Examples of typical interactions plots: upper — $I+\times I-$ antisynergistic interaction; lower — $I-\times t-$ synergistic interaction.

Table 4
Parametric responses from the experiments

Run	W^a (mm)	P^b (mm)	FA[c] (mm^2)	SZWnet[d] (mm)	GRADE[e]
1	5.0	0.5	1.2	15.4	0
2	3.4	0.4	0.5	10.2	1
3	3.1	0.4	0.9	6.4	2
4	4.1	0.6	1.2	1.1	2
5	5.3	1.3	4.1	3.7	2
6	7.7	1.4	6.0	8.9	1
7	4.0	0.7	1.6	5.8	2
8	3.2	0.4	0.6	7.3	0
9	5.3	1.2	3.8	4.0	1
10	3.2	0.4	0.9	9.3	0
11	11.2	3.1	24.3	5.3	0
12	7.3	1.9	8.1	3.5	1
13	4.4	1.0	2.8	1.1	2
14	4.8	1.0	2.9	4.0	2
15	4.5	0.0	0.0	12.5	0
16	6.3	0.7	2.0	11.1	0
3B′	3.89	0.43	0.64	4.52	
3B″	3.85	0.49	0.90	4.28	
3B‴	4.06	0.55	1.11	3.81	
6B	7.6	1.4	6.3	7.4	0
12B	5.0	1.0	2.8	6.0	2
14B	4.8	1.2	4.3	2.2	2
14C	4.7	1.3	4.7	2.2	2
14D	4.9	1.4	5.4	1.4	2
16B	4.6	0.8	2.1	5.5	1
16C	7.7	1.0	4.0	10.9	0
20	3.9	0.5	1.2	7.8	1
20B	0.0	0.0	0.0	10.4	1
20C	0.0	0.0	0.0	8.3	2

[a] W is the bead width.
[b] P is the bead penetration.
[c] FA is the fusion area (transverse bead area).
[d] SZWnet is the sputtering zone width decreased by the bead width (net).
[e] GRADE is the subjective grade based on the operator's feelings and visual observations.

Table 5
Summary of the variance analysis of the data from runs 1 to 16[a]

Responses	Factors											
	$I+$ (A)			$I-$ (A)			$t-$ (ms)			TS (cm/min)		
	F^b	Sig.[c]	Tend[d]	F	Sig.	Tend	F	Sig.	Tend	F	Sig.	Tend
W	1.2	No	No	*13.1*	*5%*	*D*	*6.7*	*5%*	*D*	***17.6***	***1%***	***I***
P	0.4	No	No	*9.0*	*5%*	*D*	*6.3*	*5%*	*D*	2.7	No	I
FA	1.8	No	D[e]	*6.5*	*5%*	*D*	3.4	No	D	3.1	No[f]	I[g]
SZWnet	0.6	No	D	2.1	No	I	12.3	5%	I	7.2	5%	I
GRADE	1.0	No	No	5.0	No	I	***13.0***	***1%***	***D***	8.0	5%	D
$V+$	*8.7*	*5%*	*D*	2.8	No	I	***19.9***	***1%***	***I***	5.6	No	No
$V-$	2.4	No	I	*8.3*	*5%*	*D*	***18.2***	***1%***	***D***	0.4	No	No

[a] Italicized values are the significant factors; bold italicized values are the most significant.
[b] F is the F-number (the higher the F, the more the influence of the factor).
[c] Sig. is the F-number significance in % (1% means high significance; 5% good significance).
[d] T end is the correlation tendency.
[e] D is the direct proportional.
[f] I is the inverse proportional).
[g] No is no defined tendency or a tendency that is not statistically significant.

Table 6
Actual responses from the experiments vs. estimate values for the supplementary runs

Run	W (mm)		P (mm)		FA (mm²)		SZWnet (mm)		GRADE	
	Actual[a]	Estim.[b]	Actual	Estim.	Actual	Estim.	Actual	Estim.	Actual	Estim.
6B	7.6	7.7	1.4	1.5	6.3	6.7	7.4	8.3	0	1
12B	5.0	6.0	1.0	1.1	2.8	5.4	6.0	6.2	2	2
20	3.9	4.1	0.5	0.7	1.2	2.9	7.8	7.4	1	1
20B	0.0	1.3	0.0	−0.5	0.0	−5.4	10.4	10.1	1	1
20C	0.0	2.1	0.0	−0.1	0.0	−4.1	8.3	6.8	2	2

[a] Actual is the measured value in the test plate.
[b] Estim. is the estimated value at 95% of confidence.

actions were of synergistic type, but some presented some antisynergistic mode (see more details in [11]).

However, the interaction assessment by plots can be misleading, since it does not show clearly the amplitude of the influence of the possible interactions. The only way to verify how much the interactions would affect the additivity of the factors is through validation, i.e., to predict the results for a chosen response (still using Taguchi's approach), assuming that the main factors are additive, and to compare them with experimental results from supplementary runs. Table 6 presents this comparison, for which the runs were picked from amongst those supplementary runs having settings that were in the range of the settings used in the experimental design (series.run 1–16).

As one can see, there is a very good agreement between estimated and actual values, except for the geometric responses from runs 20B to 20C. In these runs there were no plate fusion (no bead), a feature that only occurred partially once in the runs used in the modeling (run 15). The numerical agreement was not very close for FA also. One can infer that the main factors ($I+$, $I-$, TS and $t-$) present the desired additivity and that the approach can be used to estimate the influence of each factor in the responses.

Therefore, using again Table 5, the statistically significant results show that increase of the $t-$ is followed by an increase in arc stability (shorter SZWnet), W and P. The increase of TS is also seen to favor the arc stability and to reduce the bead width. No effect significant is expected on P. Concerning $I-$, its effect appears on the bead geometry; an augment of the $I-$ amplitude makes the bead wider and deeper. The same effect was not evident for $I+$. Both $I-$ and $I+$ seem not to affect arc stability.

4. Discussion

The results presented so far (the effect of estimation of the factors over the responses) agree thoroughly with and confirmed the results of previous work [10], even considering the differences in conditions such as no use of joint and wire feeding. Comparing the responses presented in Table 4, one can see that the decrease of $I-$ (run 20B with run 20) led to a significant reduction in P, W, and FA, but to a small increase in SZWnet (no change in GRADE). This result agrees also with those from the prediction analysis.

Observing the output from run 3B (3B′, 3B″, and 3B‴), one can observe a small increase in W, P, and FA and a small decrease in SWZnet as $I+$ was reduced. Barhorst's [8] results also showed an increase of the sputtering zone width with the increase of $I+$ (although a stronger influence than that presented in the current work). Barhorst worked with a much longer polarity time (8 ms DCEP and 8 ms DCEN), period that were long enough to bring up the $I+$ effect. Reis [10], on the other hand, observed a bead geometry reduction as $I+$ became lower. Besides the fact that the variation amongst the geometric responses is very small (within 0.1 mm), the reason for this disagreement can be the thermal stabilization of the plate along the weld (the conditions changing progressively from 3B′ to 3B‴). A prediction from Table 5 would be inconclusive, since the effect of $I+$ on the geometry showed to be statistically insignificant. Therefore, the effect of $I+$ deserves further investigation.

The effect of the duration of the electrode with negative polarity was studied more exhaustively in the present work, through runs 20B, 20C, 14B, 14C, and 14D. By comparing runs 20B ad 20C, a small increase in $t-$ (from 4.7 to 8.7 ms) did not improve penetration, despite having provided better arc stability (a narrower SZWnet). This observation is in entire agreement with previous work [10], in which the effect of $t-$ on the geometry appeared only for longer $t-$. In the series 14B–14D, considering also run 14, the effect is very evident: increasing P and decreasing SZWnet as $t-$ becomes longer. W seems not to alter. It is important to note that this variation, however, is asymptotic, i.e., it has the increment progressively shortened for longer $t-$. As very long negative times seem to produce oxides on the bead, a balance between a deep penetration and a cleaned bead should be pursued during parameters setting.

A contradictory point about the results of this work results is that Barhorst found an increase in the SZW with the variation of $t-$ from 2 to 8 ms. The findings of Norrish and Ooi [7] are also noteworthy: for fully penetrated welds on thin plate, the weld bead decreases with increasing electrode negative cycle. This observation is supported by the results from one part of previous work [10] and disagrees with the prediction shown in Table 5 and the results from Table 4.

However, Norrish and Ooi worked at a frequency of around 200 Hz and in the first part of the previous work a frequency range of 125–200 Hz was employed. In the second part of the previous work, with longer $t-$ (a cycle frequency of around 45–150 Hz), increased $t-$ caused no significant change in W. In the current work, the frequency was also varied between approximately 45 and 150 Hz, reaching the range of 24–38 Hz for run 14A–14C series.

The effect of TS observed in Table 5 was checked through run 16B, which had the TS doubled in relation to that of run 16. As seen in Table 4, both W and SZWnet had their values significantly reduced: notwithstanding, P did not alter. That was exactly what was predicted in Table 5. TS had also shown in previous work [10] a not very significant effect on P, but a very significant effect on W. Its effect on stability was also noticed. Lancaster [2] had also noticed the reduction of the sputtered zone width with an increasing TS. This weak effect of TS on penetration may be connected to the high heat transfer coefficient of aluminum.

Concerning the electrode positive duration, run 16C was made with a longer $t+$ in relation to run 16. Table 4 shows an unexpected improvement in the geometric parameters (a wider and deeper bead). SZWnet did not change significantly. This effect was not observed in previous work [10], in which the $t+$ effect on geometry was insignificant (the plate composition was rather different). Norrish and Ooi [7] observed an increase of the sputtering zone width for increasing $t+$ only for low currents. Therefore, a further study of the plate condition and current level influences on the $t+$ setting seems to be demanded.

Table 5 also suggests a very significant influence of $t-$ on arc voltage; the longer the $t-$, the higher the $V-$ and lower the $V+$. $V-$ and $V+$ are also raised if $I-$ and $I+$, respectively, are increased. An interesting observation in the voltage traces was a voltage growth tendency during the $t-$ fraction time. This phenomenon, illustrated in Fig. 2, is regardless the $t-$ setting. These facts may be connected to a poor oxygen pick-up. If on one hand the oxide helps the of field emission during positive polarity (less $V+$), and consequently the cathodic self-cleaning phenomenon, on the other hand it makes it more difficult to tougher the electron to go into the plate during negative polarity (higher $V-$). However, the main reason for this phenomenon is probably base on a reduction in the electrode temperature along the negative period (the electrode is heated up during the positive period), making more difficult the thermoionic emission.

The influence of current amplitude ($I+$ or $I-$), TS and $t-$ on the weld geometry can be explained by the heat delivery onto the plate: it is widely known that in GTAW the thermal efficiency is much higher with negative polarity than with positive polarity. The beneficial action of bigger $t-$ and TS on the arc stability deserves further explanation. A hypothesis would be that for long $t-$, there would be proportionally less time on oxide cleaning ($t+$) and more time for oxide formation, which are responsible for the cathodic emission (as long as $t-$ is not so lengthy as to create an oxide barrier to the electrons). A slower TS will in practice increase the time that a portion of the weld pool will be under the action of the oxide cleaning (an even shorter $t+$ is expected to improve the arc stability of slow welding). The process seems to work in such a way that when the electrode is with negative polarity, the electron emission is governed by the thrmoionic mechanism. The required voltage I not very high and the heat transfer to the plate is efficient. However, the oxide rising on the plate will disturb the heat transfer for the plate. After changing to the positive polarity, the electron emission becomes controlled by the field emission mechanism, which requires some oxides on the plate and a higher voltage. This oxide is prone to come from the reaction of the plate elements with some residual oxygen in the arc environment (a plate previously heated showed better arc starting). This emission process is self-degenerating, since it destroy its own source. A long $t+$ may provide excessive oxide clean-

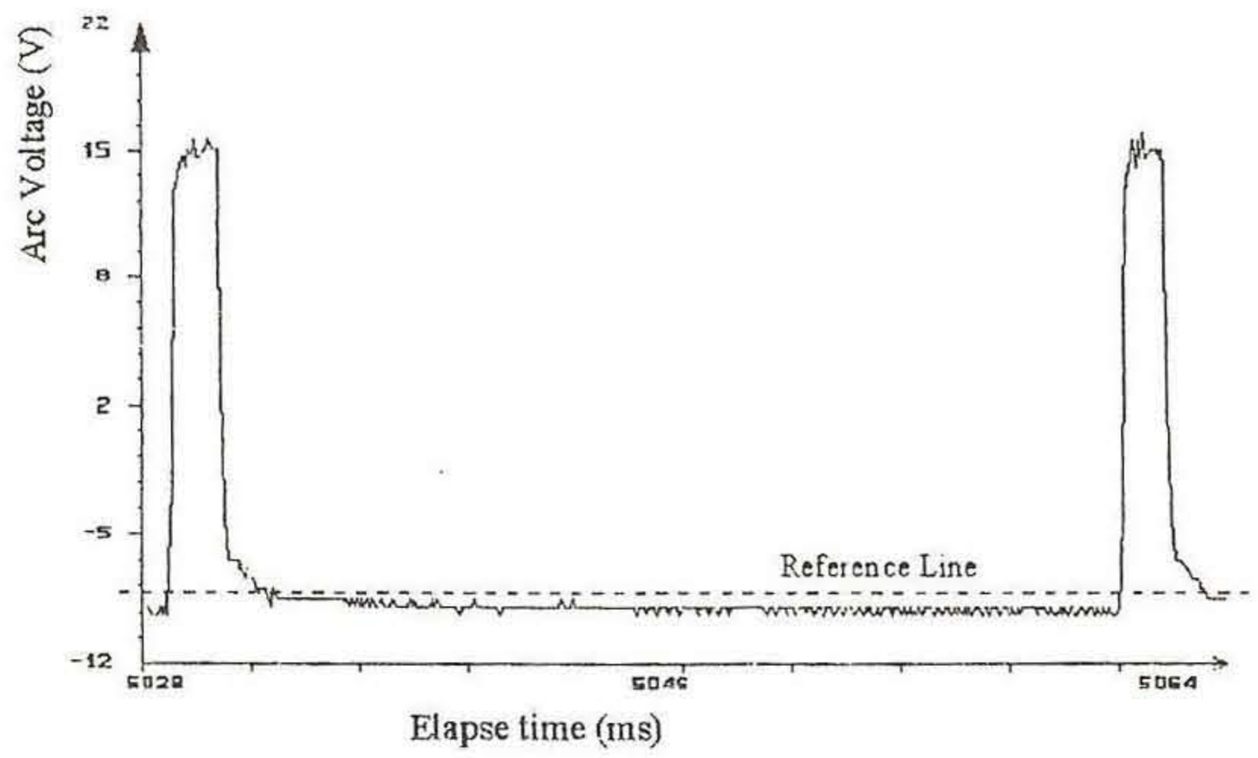

Fig. 2. A segment of the voltage trace of the CP14D ($t-$=30 ms). It can be noted by the reference line that the voltage increases along the elapsed time within the negative period.

ness on the cathode (plate) and the field emission can be interrupted. Evidence of this is that in CA sinusoidal (50–60 Hz, $t+=t-$), the HF overlap signal needs to be enabled during the entire cycle. The transition from the positive to the negative polarity is less dramatic, since the electrode is already hot and able to emit electrons. On the contrary, the transition from the negative to positive polarity demands the presence of some oxide and the help of a high voltage transient for the re-striking.

From the analyses, one can draw a conclusion that the cathodic self-cleaning phenomena can be beneficial or detrimental to the weld, since insufficient oxide cleaning can lead to inadequate bead formation, whereas complete oxide cleaning favors arc instability.

5. Conclusions

For the aluminum under study, the following conclusions were drawn:

1. The selection of welding parameters must accomplish both arc stability and bead formation altogether.
2. The control of the governing factors on the cathodic self-cleaning phenomenon (positive electrode duration and polarity reversal frequency) can lead to a good compromise between arc stability and bead formation.
3. A 2 ms long positive electrode duration time seems to be enough for the cathodic self-etching action, but the parameter setting must take into account the need of an appropriate elapsed time between two periods of weld with the electrode in positive polarity. There must be some oxide layer on the weld pool or on the plate ahead before the polarity reversal (from negative to positive) to ensure arc stability.
4. This stability is reached with a faster travel speed and a sufficiently long negative duration time. The setting value limits (lower and upper) will depend on the plate composition and condition (the degree of oxidation). Too fast a travel speed will reduce the bead size, whilst too long a negative duration time will increase it, but the weld bead becomes prone to oxidation.
5. The geometry can still be controlled by negative electrode amplitude, the setting of which does not affect the cathodic self-cleaning phenomenon.

References

[1] P.G. Jönsson, A.B. Murphy, J. Szekely, The influence of oxygen additions on argon-shielded GMAW processes, Welding. J. AWS (1995) 48s–58s.
[2] J.P. Lancaster, The Physics of Welding, 1st Edition, Pergamon Press, Oxford, 1984, p. 115, 153, 156, 157 (Chapter 5 and 6) (ISBN 0-08-030554-7).
[3] AWS, Welding Handbook — Vol. II: Welding Process, 8th Edition, AWS, 1991, pp. 74–107 (Chapter 3).
[4] S. Anik, L. Dorn, Metal-physical process involved in welding — welding of aluminium materials, Welding Res. Abroad XXXVIII (3) (1992) 36–41.
[5] J.P. Lancaster, The physics of fusion welding — Part 1: the electric arc in welding, IEE Proc. 134(5) (1987) 233–252.
[6] P.J. Modenesi, J.H. Nixon, Arc instability phenomena in GMAW, Welding J. AWS (1994) 219s–224s.
[7] J. Norrish, C.L. Ooi, Adaptive asymmetric waveform control in bipolar gas tungsten arc welding of aluminium, Welding Met. Fab. (1993) 230–232.
[8] S. Barhorst, The cathodic etching technique for automated aluminum tube welding, Welding J. AWS (1985) 28–31.
[9] D. Rehfeldt, T. Schimitz, H. Mecke, Döbbelin, D. Heyder, Studies into the use of higher frequencies for tungsten-inert gas welding with low alternating currents, Welding and Cutting 5 (1996) E90–E93.
[10] R.A. Reis, Determination of welding parameters for TIG with cold wire and rectangular wave output, M.Sc. Thesis, Universidade Federal de Uberlandia, Brazil, 1996 (in Portuguese).
[11] A. Scotti, A study on the effect of the setting parameters on the arc stability and bead geometry of aluminum GTAW using asymmetric rectangular wave AC output, Internal Research Report Laprosolda No. 14/96, UFU, Brazil, 1996.
[12] M.S. Phadke, Quality Engineering Using Robust Design, Prentice-Hall, Englewood Cliffs, NJ, 1989, pp. 51–59, 63, 154 (Chapter 7) (ISBN 0-13-745167-9).